ANALYSIS OF THE TURKEL-ZWAS SCHEME FOR THE TWO-DIMENSIONAL SHALLOW WATER EQUATIONS IN SPHERICAL COORDINATES

B. Neta *†
Department of Mathematics
Naval Postgraduate School
Code MA/Nd
Monterey, California 93943

F. X. Giraldo ‡
NRC Research Associate
Department of Mathematics
Naval Postgraduate School
Monterey, California 93943

I.M. Navon
Department of Mathematics
and
Supercomputer Computations Research Institute
Florida State University
Tallahassee, FL 32306

November 28, 1995

---

*Part of this research was conducted while the author was visiting the Department of Mathematics at the Technion, Haifa, Israel.

†Author to whom correspondence should be addressed.

‡Current address: Naval Research Laboratory, Monterey, CA 93940

KEYWORDS: shallow water equations; finite differences; Turkel-Zwas scheme; spherical coordinates; stability analysis.

SUMMARY

A linear analysis of the shallow water equations in spherical coordinates for the Turkel-Zwas (T-Z)[1] explicit large time-step scheme is presented. This paper complements the results of Schoenstadt,[2] Neta and Navon[3] and others in 1-D, and of Neta and DeVito[4] in 2-D, but applied to the spherical coordinate case of the T-Z scheme. This coordinate system is more realistic in meteorology and more complicated to analyze, since the coefficients are no longer constant. The analysis suggests that the T-Z scheme must be staggered in a certain way in order to get eigenvalues and eigenfunctions approaching those of the continuous case. The importance of such an analysis is the fact that it is also valid for non-constant coefficients and thereby applicable to any numerical scheme. Numerical experiments comparing the original (unstaggered) and staggered versions of the T-Z scheme are presented. These experiments corroborate the analysis by showing the improvements in accuracy gained by staggering the Turkel-Zwas scheme.

1 INTRODUCTION

The transfer function was first introduced in electrical engineering by Stremler[7]. This is different from Fourier analysis since it gives information about amplitude distortion and not just phase. Schoenstadt[2] has applied the idea to compare various schemes for the one-dimensional shallow water system. Neta and Navon[3] extended the results to include the Turkel-Zwas[1] explicit large time-step scheme on a limited-area domain for the shallow water equations. Steppeler[8–9] analyzed some hybrid methods. Neta and DeVito[4] extended Schoenstadt's results to the two-dimensional case. Neta[10] has extended the transfer function analysis to the two dimensional Turkel-Zwas explicit large time-step finite difference scheme in a Cartesian coordinate system. Song and Tang[13] have used Laplace transform instead of Fourier to analyze the unstaggered ans well as the staggered Turkel-Zwas scheme.

In this paper we extend the linear transfer function analysis to the two dimensional shallow water equations in spherical coordinates for the Turkel-Zwas discretization. Actually, we show how to obtain modal expansion for the shallow water equations in spherical coordinates and for the Turkel Zwas discretization of these equations. At this point, we should comment on the choice of the method. Computationally efficient and accurate schemes for the numerical solution of the shallow water equations are of crucial importance in atmospheric and oceanographic models. Two different approaches have been taken, both of them dealing with the different time scales of the advective (Rossby) waves and the gravity inertia waves separately. The first of these was the split-explicit and semi-implicit schemes. The Turkel-Zwas scheme takes a different view by proposing a space (rather than time) splitting approach. This is based on the fact that the fast gravity inertia waves which restrict the time step contain only a small fraction of the total available energy and therefore can be calculated with a lower accuracy on a coarse grid. The Rossby waves which contain most of the energy are calculated on the finer mesh. When the ratio of the coarse and fine grids is an integer $p > 1$, one can use time steps nearly p times larger than those allowed by the usual explicit scheme. The CFL condition for the Turkel Zwas scheme on a rectangular domain can be found in Turkel-Zwas[1] and Song and Tang[13]. For spherical coordinated, the CFL condition is given in Navon and deVilliers[5]

$$\Delta t \leq \frac{a \cos \theta}{\sqrt{gH}} \frac{p \Delta \lambda}{\sin pk \Delta \lambda}.$$

The importance of this explicit scheme is also in parallelization. It is always easier to use an explicit scheme on parallel computers and certainly these modifications and the analysis will encourage the development of a parallel Turkel-Zwas scheme.

In section 2 we present the modal expansion for the linearized shallow water equations with no mean flow in spherical coordinates. We start (subsection 2.1) by obtaining the linearization of the shallow water equations on the sphere. Then (subsection 2.2) describe the modal expansion for the linearized system as obtained by Longuet-Higgins[12]. In section 3 we present the modal expansion for the linearized shallow water equations in spherical coordinates discretized using the Turkel-Zwas finite difference scheme. We start this section by describing the Turkel-Zwas scheme (subsection 3.1). The modal expansion is given in subsection 3.2 and the last subsection provides a comparison of exact and discrete modal expansions. As a result of this analysis, we conclude that certain staggering is necessary. A modified staggered method, different from those suggested by Song and Tang[13], is given in section 4. In section 5 we present the numerical results of this study showing the benefits gained by staggering the Turkel-Zwas scheme for the shallow water equations, and in section 6 we give the concluding remarks.

2 SHALLOW WATER EQUATIONS

2.1 Linearization

The shallow water equations in spherical coordinates are given by

$$\frac{\partial u}{\partial t} + \frac{1}{a\cos\theta}\left[u\frac{\partial u}{\partial \lambda} + v\cos\theta\frac{\partial u}{\partial \theta}\right] - (f + \frac{u}{a}\tan\theta)v + \frac{g}{a\cos\theta}\frac{\partial h}{\partial \lambda} = 0 \tag{1}$$

$$\frac{\partial v}{\partial t} + \frac{1}{a\cos\theta}\left[u\frac{\partial v}{\partial \lambda} + v\cos\theta\frac{\partial v}{\partial \theta}\right] + (f + \frac{u}{a}\tan\theta)u + \frac{g}{a}\frac{\partial h}{\partial \theta} = 0 \tag{2}$$

$$\frac{\partial h}{\partial t} + \frac{1}{a\cos\theta}\left[\frac{\partial}{\partial \lambda}(hu) + \frac{\partial}{\partial \theta}(hv\cos\theta)\right] = 0\ . \tag{3}$$

Here, f is the Coriolis parameter given by

$$f = 2\Omega\sin\theta \tag{4}$$

where Ω is the angular speed of the rotation of the earth, h is the height of the homogeneous atmosphere, u and v are the zonal and meridional wind components respectively, θ and λ are the latitudinal and longitudinal directions respectively, a is the radius of the earth, and g is the gravitational constant.

The two-dimensional linearized shallow water equations (LSW) with no mean flow in spherical coordinates are

$$\frac{\partial u}{\partial t} - fv + \frac{g}{a\cos\theta}\frac{\partial h}{\partial \lambda} = 0 \tag{5}$$

$$\frac{\partial v}{\partial t} + fu + \frac{g}{a}\frac{\partial h}{\partial \theta} = 0 \tag{6}$$

$$\frac{\partial h}{\partial t} + \frac{H}{a\cos\theta}\left(\frac{\partial u}{\partial \lambda} + \frac{\partial}{\partial \theta}(v\cos\theta)\right) = 0, \tag{7}$$

where H is the mean height of the surface and h is the perturbation. In the next subsection we describe the modal expansion given by Longuet-Higgins[12].

2.2 Modal Expansion to the LSW (Longuet-Higgins)

It can be shown (Pedlosky[11]) that for <u>constant</u> f (e.g. mean value in the case of a limited area model) the system (5)-(7) is equivalent to

$$\frac{\partial^3 h}{\partial t^3} + f^2 \frac{\partial h}{\partial t} - \frac{gH}{a^2} \nabla^2 \left(\frac{\partial h}{\partial t} \right) = 0 \; . \tag{8}$$

Let

$$h(t, \lambda, \mu) = H_0 e^{-ict} e^{im\lambda} P_{\rm mn}(\mu) \tag{9}$$

where $P_{\rm mn}(\mu)$ are the associated Legendre polynomials and

$$\mu = \sin\theta \tag{10}$$

then

$$\frac{\partial^3 h}{\partial t^3} + \left[f^2 + \frac{n(n+1)gH}{a^2} \right] \frac{\partial h}{\partial t} = 0 \tag{11}$$

and the frequency c can take the values

$$c = 0, \pm\omega \tag{12}$$

where

$$\omega = \sqrt{f^2 + \frac{gH}{a^2} n(n+1)} \; . \tag{13}$$

For the case of interest here, f is <u>not</u> constant (i.e. given by (4)), and (8) is no longer valid. Thus the eigenfunctions and eigenvalues are no longer given by (9) and (12) respectively. In order to obtain the eigenpairs, <u>we follow the discussion in Longuet-Higgins[12]</u> on Laplace's tidal equations, which are (5)-(7). We should remark here that the variable θ in Longuet-Higgins[12] is $\frac{\pi}{2} - \theta$. We seek periodic solutions to (5)-(7) which are proportional to $e^{i(m\lambda - ct)}$ where m is a non negative integer and c a constant non zero frequency. Substituting such an exponential in (5)-(7), we get im instead of $\frac{\partial}{\partial\lambda}$, and $-ic$ instead of $\frac{\partial}{\partial t}$. Now solve (5)-(6) for u and v in terms of h, we get

$$u = \frac{g}{a} \frac{1}{2\Omega(\Lambda^2 - \sin^2\theta)} \left[\frac{m\Lambda}{\cos\theta} + \sin\theta \frac{\partial}{\partial\theta} \right] h \tag{14}$$

and

$$v = \frac{g}{a} \frac{-i}{2\Omega(\Lambda^2 - \sin^2\theta)} \left[\frac{m}{\cot\theta} + \Lambda \frac{\partial}{\partial\theta} \right] h \tag{15}$$

where

$$\Lambda = \frac{c}{2\Omega}, \tag{16}$$

a non dimensional frequency. Substituting for u and v in (7) we have

$$\mathcal{L}h = \epsilon h \tag{17}$$

where the operator $\mathcal{L}$ denotes the linear operator

$$\mathcal{L} \equiv \frac{1}{\Lambda \cos\theta}\left[\frac{\partial}{\partial\theta}\left\{\frac{-1}{\Lambda^2 - \sin^2\theta}\left(m\sin\theta + \Lambda\cos\theta\frac{\partial}{\partial\theta}\right)\right\} + \frac{m}{\Lambda^2 - \sin^2\theta}\left(\frac{m\Lambda}{\cos\theta} + \sin\theta\frac{\partial}{\partial\theta}\right)\right] \tag{18}$$

and where (Lamb's parameter, ϵ) is given by

$$\epsilon = \frac{4\Omega^2 a^2}{gH}. \tag{19}$$

The problem then reduces to finding functions h, finite and with continuous derivatives in $-\frac{\pi}{2} \leq \theta \leq \frac{\pi}{2}$, ans also pairs of constants Λ and ϵ so as to satisfy (17).

Longuet-Higgins[12] suggested two methods of solution. In the first, functions analogous to the velocity potential (Φ) and stream function (Ψ) are introduced, such that

$$u = \frac{1}{\cos\theta}\frac{\partial\Phi}{\partial\lambda} + \frac{\partial\Psi}{\partial\theta} \tag{20}$$

$$v = \frac{\partial\Phi}{\partial\theta} - \frac{1}{\cos\theta}\frac{\partial\Psi}{\partial\lambda}. \tag{21}$$

Then $\nabla^2\Phi$, $\nabla^2\Psi$ are the divergence and vorticity, where ∇^2 denotes the horizontal Laplacian operator,

$$\nabla^2 = \frac{1}{\cos\theta}\left[\frac{\partial}{\partial\theta}\left(\cos\theta\frac{\partial}{\partial\theta}\right) + \frac{1}{\cos\theta}\frac{\partial^2}{\partial\lambda^2}\right]. \tag{22}$$

Longuet-Higgins has shown that

$$\frac{\partial}{\partial t}\nabla^2\Phi + 2\Omega\sin\theta\nabla^2\Psi + 2\Omega\cos\theta u + \frac{g}{a}\nabla^2 h = 0 \tag{23}$$

$$\frac{\partial}{\partial t}\nabla^2\Psi - 2\Omega\sin\theta\nabla^2\Phi - 2\Omega\cos\theta v = 0. \tag{24}$$

Equation (7) can also be written

$$\frac{\partial h}{\partial t} + \frac{H}{a}\nabla^2\Phi = 0. \tag{25}$$

Substituting for u and v from (20)-(21) to get

$$\left(\frac{\partial}{\partial t}\nabla^2 + 2\Omega\frac{\partial}{\partial\lambda}\right)\Phi + 2\Omega\left(\sin\theta\nabla^2 + \cos\theta\frac{\partial}{\partial\lambda}\right)\Psi = -\frac{g}{a}\nabla^2 h \tag{26}$$

$$\left(\frac{\partial}{\partial t}\nabla^2 + 2\Omega\frac{\partial}{\partial\lambda}\right)\Psi - 2\Omega\left(\sin\theta\nabla^2 + \cos\theta\frac{\partial}{\partial\lambda}\right)\Phi = 0. \tag{27}$$

We seek solutions to these equations (25)-(27) which shall be proportional to $e^{i(m\lambda - ct)}$, where m is a non negative integer and c denotes the radian frequency. For convenience we use the operator D as

$$D = (1-\mu^2)\frac{\partial}{\partial\mu}.$$

Then equations (25)-(27) become

$$\left(\Lambda\nabla^2 - m\right)\Phi + \left(\mu\nabla^2 + D\right)i\Psi = -\frac{ig}{2\Omega}\nabla^2 h \tag{28}$$

$$\left(\Lambda\nabla^2 - m\right)i\Psi + \left(\mu\nabla^2 + D\right)\Phi = 0 \tag{29}$$

$$ich = \frac{H}{a}\nabla^2\Phi \tag{30}$$

where now

$$\nabla^2 \equiv \frac{d}{d\mu}\left[(1-\mu^2)\frac{d}{d\mu}\right] - \frac{m^2}{1-\mu^2}.$$

Upon eliminating h from (28) and (30) we get

$$\left(\Lambda\nabla^2 - m + \frac{a^2}{\epsilon\Lambda}\nabla^4\right)\Phi + \left(\mu\nabla^2 + D\right)i\Psi = 0. \tag{31}$$

The functions Φ and Ψ are expanded in spherical harmonics and the eigenvalues are computed by solving **two** systems of algebraic equations

$$\det\left(\Lambda I - C - \frac{1}{\epsilon\Lambda}J\right) = 0$$

$$\det\left(\Lambda I - C - \frac{1}{\epsilon\Lambda}J'\right) = 0$$

where C is a tridiagonal matrix, I is the identity matrix and J and J' are diagonal (see (3.26), (3.27) and (3.29) in Longuet-Higgins.) The solution of the first gives the frequencies of the normal modes.

In the next chapter, we follow a similar derivation for the semi-discretization given by the Turkel-Zwas scheme. It should be noted that the idea can applied to **any** numerical (semi-discrete) scheme. We will show how equations (28)-(31) will be affected by the discretization and prove that staggering is necessary.

3 TURKEL-ZWAS SCHEME

3.1 Discretization

Given a constant α, $0 < \alpha \leq 1$, the Turkel-Zwas scheme for the nonlinear shallow water equations in spherical coordinates takes the following form:

$$
\begin{aligned}
u_{k,j}^{\ell+1} = u_{k,j}^{\ell-1} \quad & -\sigma\left[\tfrac{u_{k,j}^{\ell}}{\cos\theta_j}(u_{k+1,j}^{\ell} - u_{k-1,j}^{\ell}) + v_{k,j}^{\ell}(u_{k,j+1}^{\ell} - u_{k,j-1}^{\ell})\right. \\
& \left. + \tfrac{g}{p\cos\theta_j}(h_{k+p,j}^{\ell} - h_{k-p,j}^{\ell})\right] \\
& + 2\Delta t\left[(1-\alpha)(f_j + \tfrac{u_{k,j}^{\ell}}{a}\tan\theta_j)v_{k,j}^{\ell}\right. \\
& + \tfrac{\alpha}{2}(f_j + \tfrac{u_{k+p,j}^{\ell}}{a}\tan\theta_j)v_{k+p,j}^{\ell} \\
& \left. + \tfrac{\alpha}{2}(f_j + \tfrac{u_{k-p,j}^{\ell}}{a}\tan\theta_j)v_{k-p,j}^{\ell}\right]
\end{aligned}
\tag{32}
$$

$$
\begin{aligned}
v_{k,j}^{\ell+1} = v_{k,j}^{\ell-1} \quad & -\sigma\left[\tfrac{u_{k,j}^{\ell}}{\cos\theta_j}\left(v_{k+1,j}^{\ell} - v_{k-1,j}^{\ell}\right) + v_{k,j}^{\ell}\left(v_{k,j+1}^{\ell} - v_{k,j-1}^{\ell}\right)\right. \\
& \left. + \tfrac{g}{q}\left(h_{k,j+q}^{\ell} - h_{k,j-q}^{\ell}\right)\right] \\
& - 2\Delta t\left[(1-\alpha)\left(f_j + \tfrac{u_{k,j}^{\ell}}{a}\tan\theta_j\right)u_{k,j}^{\ell}\right. \\
& + \tfrac{\alpha}{2}\left(f_{j+q} + \tfrac{u_{k,j+q}^{\ell}}{a}\tan\theta_{j+q}\right)u_{k,j+q}^{\ell} \\
& \left. + \tfrac{\alpha}{2}\left(f_{j-q} + \tfrac{u_{k,j-q}^{\ell}}{a}\tan\theta_{j-q}\right)u_{k,j-q}^{\ell}\right]
\end{aligned}
\tag{33}
$$

$$
\begin{aligned}
h_{k,j}^{\ell+1} = h_{k,j}^{\ell-1} \quad & -\sigma \left\{ \tfrac{u_{k,j}^{\ell}}{\cos\theta_j} \left(h_{k+1,j}^{\ell} - h_{k-1,j}^{\ell} \right) + v_{k,j}^{\ell} \left(h_{k,j+1}^{\ell} - h_{k,j-1}^{\ell} \right) \right. \\
& + \tfrac{h_{k,j}^{\ell}}{\cos\theta_j} \left[(1-\alpha) \left(u_{k+p,j}^{\ell} - u_{k-p,j}^{\ell} \right) \right. \\
& \left. + \tfrac{\alpha}{2} \left(u_{k+p,j+q}^{\ell} - u_{k-p,j+q}^{\ell} + u_{k+p,j-q}^{\ell} - u_{k-p,j-q}^{\ell} \right) \right] \tfrac{1}{p} \\
& + \tfrac{h_{k,j}^{\ell}}{\cos\theta_j} \left[(1-\alpha) \left(v_{k,j+q}^{\ell} \cos\theta_{j+q} - v_{k,j-q}^{\ell} \cos\theta_{j-q} \right) \right. \\
& + \tfrac{\alpha}{2} \left(v_{k+p,j+q}^{\ell} \cos\theta_{j+q} - v_{k+p,j-q}^{\ell} \cos\theta_{j-q} \right. \\
& \left. \left. \left. + v_{k-p,j+q} \cos\theta_{j+q} - v_{k-p,j-q} \cos\theta_{j-q} \right) \right] \tfrac{1}{q} \right\}
\end{aligned}
\tag{34}
$$

where

$$
\sigma = \frac{\Delta t}{a \Delta\lambda} = \frac{\Delta t}{a \Delta\theta}. \tag{35}
$$

We note that the λ, θ components of the pressure gradient and diveregnce terms are differenced over points, $p\Delta\lambda$, $q\Delta\theta$ (respectively) away rather than nearest neighbors. This way, the terms associated with the gravity waves (which carry little energy) can be approximated less accurately and thus allowing a larger time step. For $\alpha = 0$, Turkel and Zwas showed that there is a deterioration of accuracy for p larger than one. For $\alpha = \frac{1}{3}$ the geostrophic balance and the incompressibility condition are satisfied to a higher order in the Cartesian coordinate case (See Turkel and Zwas,[1] Navon and de Villiers[5] and Navon and Yu[6]). For the spherical coordinates case, again Turkel and Zwas show that the choice $\alpha = \frac{1}{3}$ was necessary to preserve accuracy when p or q is greater than one.

The Turkel-Zwas scheme for the approximation of (5)-(7) can be written as

$$
\left.\frac{\partial u}{\partial t}\right|_{k,j} = -\frac{1}{2a\Delta\lambda} \, \frac{g}{p\cos\theta_j} \left(h_{k+p,j} - h_{k-p,j} \right) + f_j \left[(1-\alpha) v_{k,j} + \frac{\alpha}{2} \left(v_{k+p,j} + v_{k-p,j} \right) \right] \tag{36}
$$

$$
\left.\frac{\partial v}{\partial t}\right|_{k,j} = -\frac{1}{2a\Delta\theta} \, \frac{g}{q} \left(h_{k,j+q} - h_{k,j-q} \right) - \left[(1-\alpha) f_j u_{k,j} + \frac{\alpha}{2} \left(f_{j+q} u_{k,j+q} + f_{j-q} u_{k,j-q} \right) \right] \tag{37}
$$

$$
\begin{aligned}
\left.\frac{\partial h}{\partial t}\right|_{kj} = & -\frac{1}{2a}\frac{H}{\cos\theta_j}\left[(1-\alpha)\left(\frac{u_{k+p,j}-u_{k-p,j}}{p\Delta\lambda}+\frac{v_{k,j+q}\cos\theta_{j+q}-v_{k,j-q}\cos\theta_{j-q}}{q\Delta\theta}\right)\right. \\
& +\frac{\alpha}{2}\left(\frac{u_{k+p,j+q}-u_{k-p,j+q}}{p\Delta\lambda}+\frac{u_{k+p,j-q}-u_{k-p,j-q}}{p\Delta\lambda}\right. \\
& +\frac{v_{k+p,j+q}\cos\theta_{j+q}-v_{k+p,j-q}\cos\theta_{j-q}}{q\Delta\theta} \\
& \left.\left.+\frac{v_{k-p,j+q}\cos\theta_{j+q}-v_{k-p,j-q}\cos\theta_{j-q}}{q\Delta\theta}\right)\right].
\end{aligned} \tag{38}
$$

Note that there is a typographical error in equation (11a) of Turkel-Zwas[1] which is our equation (36). We have also modified (to get a symmetric approximation as suggested by Neta[9] for a rectangular domain) the right hand side of (11c) in Turkel-Zwas[1] which is (38) here.

3.2 Modal Expansion for the Discretized System

When substituting u, v, h given by

$$u = U_0 e^{i(m\lambda - ct)}\Pi^u_{mn}(\mu) \tag{39}$$

$$v = V_0 e^{i(m\lambda - ct)}\Pi^v_{mn}(\mu) \tag{40}$$

$$h = H_0 e^{i(m\lambda - ct)}\Pi_{mn}(\mu)^* \tag{41}$$

in (36) - (37) one encounters terms like

$$\Pi_{mn}(\sin\theta_{j\pm q}),\ \Pi^u_{mn}(\sin\theta_{j\pm q}),\ \Pi^v_{mn}(\sin\theta_{j\pm q}),\ \sin\theta_{j\pm q}\Pi^u(\sin\theta_{j\pm q}).$$

All these terms are expanded in Taylor series to order $(q\Delta\theta)^2$. Higher order terms are neglected. The resulting equations after lengthy algebraic manipulations performed by the help of MACSYMA are

$$-icu_{kj} = -\frac{g}{a}im\eta\frac{h_{kj}}{\cos\theta_j} + f_j\rho v_{kj} \tag{42}$$

$$-icv_{kj} = -\frac{g}{a}\frac{\partial h_{kj}}{\partial\theta} - f_j u_{kj} \tag{43}$$

---

*The functions Π_{mn}, Π^u_{mn}, and Π^v_{mn} give the eigenfunctions in μ for h, u, v respectively. See (50) later, the eigenvalue problem leading to Π_{mn}

where

$$\rho = 1 - \alpha + \alpha \cos mp\Delta\lambda \tag{44}$$

$$\eta = \frac{\sin mp\Delta\lambda}{mp\Delta\lambda}. \tag{45}$$

Equations (42) - (43) can be solved for u_{kj} and v_{kj}, thus

$$u_{kj} = \frac{g}{a}\frac{1}{2\Omega Q(\theta_j)}\left[m\Lambda\eta \sec\theta_j + \rho \sin\theta_j \frac{\partial}{\partial\theta}\right] h_{kj} \tag{46}$$

$$v_{kj} = -i\frac{g}{a}\frac{1}{2\Omega Q(\theta_j)}\left[m\eta \tan\theta_j + \Lambda\frac{\partial}{\partial\theta}\right] h_{kj} \tag{47}$$

where Λ is given by (16) and

$$Q(\theta_j) = \Lambda^2 - \rho \sin^2\theta_j. \tag{48}$$

Note that when $\Delta\lambda \to 0$, then η and ρ tend to 1 and (46)-(47) become (14)-(15). Substituting (39) - (41) in (38) and neglecting higher order terms as before one has

$$-ich_{kj} = -\frac{H}{a\cos\theta_j}\left[im\eta\, u_{kj} + \rho\frac{\partial}{\partial\theta}\left(v_{kj}\cos\theta_j\right)\right]. \tag{49}$$

Substituting (46) and the derivative of (47) with respect to θ in (49) yields the following eigenvalue problem

$$L\Pi_{mn}(\mu_j) = \epsilon\Pi_{mn}(\mu_j) \tag{50}$$

where ϵ is given by (19) and the operator L is given by

$$\begin{aligned} L\Pi_{mn}(\mu_j) = \quad & \frac{1}{\Lambda\cos\theta_j}\left[\frac{\partial}{\partial\theta}\left\{\frac{-\rho}{Q(\theta_j)}\left(m\eta\sin\theta_j + \Lambda\cos\theta_j\frac{\partial}{\partial\theta}\right)\right\}\Pi_{mn}(\mu_j)\right. \\ & \left. + \frac{m}{Q(\theta_j)}\left(\frac{m\Lambda\eta^2}{\cos\theta_j} + \eta\rho\sin\theta_j\frac{\partial}{\partial\theta}\right)\Pi_{mn}(\mu_j)\right]. \end{aligned} \tag{51}$$

This operator depends on the discretization used and it tends to $\mathcal{L}$ as given by (18) when $\Delta\lambda \to 0$. We follow the first method of Longuet-Higgins to show how the eigenvalues are computed. Now, define two functions analogous to the velocity potential and stream function such that at each point

$$u_{kj} = \frac{1}{\cos\theta_j}\delta_p\Phi_{kj} + \delta_q\Psi_{kj} \tag{52}$$

$$v_{kj} = \delta_q\Phi_{kj} - \frac{1}{\cos\theta_j}\delta_p\Psi_{kj} \tag{53}$$

which are the discrete analog of (20) - (21), where

$$\delta_p \Phi_{kj} = \frac{\Phi_{k+p/2\,j} - \Phi_{k-p/2\,j}}{p\Delta\lambda} \tag{54}$$

$$\delta_q \Phi_{kj} = \frac{\Phi_{k\,j+q/2} - \Phi_{k\,j-q/2}}{q\Delta\theta}. \tag{55}$$

It can be shown that $\nabla^2\Phi$ and $\nabla^2\Psi$ satisfy the discrete analog of (22), i.e.

$$\nabla^2\Phi_{kj} = \frac{1}{\cos^2\theta_j}\delta_p^2\Phi_{kj} + \frac{1}{\cos\theta_j}\delta_q(\cos\theta_j\delta_q\Phi_{kj}) \tag{56}$$

and similarly for Ψ.

Now combine the right hand sides of equations (36)-(37) in the following way

$$\frac{1}{\cos\theta_j}\left[\frac{(36)k+p/2\;j^{\dagger}\; - (36)k-p/2\;j}{p\Delta\lambda} + \frac{(37)k\;j+q/2\cos\theta_{j+q/2} - (37)_{k\;j-q/2}\cos\theta_{j-q/2}}{q\Delta\theta}\right].$$

After a lengthy algebraic manipulation, one has to $O\left((q\Delta\theta)^2\right)$, which agrees with (23),

$$\frac{\partial}{\partial t}\nabla^2\Phi_{kj} + 2\Omega\sin\theta_j\nabla^2\Psi_{kj} + 2\Omega\cos\theta_j u_{kj} + \frac{g}{a}\nabla^2 h_{kj} = 0\,. \tag{57}$$

Taking

$$\frac{1}{\cos\theta_j}\left[-\frac{(37)k+p/2\;j - (37)k-p/2\;j}{p\Delta\lambda} + \frac{(36)k\;j+q/2\cos\theta_{j+q/2} - (36)_{k\;j-q/2}\cos\theta_{j-q/2}}{q\Delta\theta}\right]$$

one has (note the similarity to (24))

$$\frac{\partial}{\partial t}\nabla^2\Psi_{kj} - 2\Omega\sin\theta_j\nabla^2\Phi_{kj} - 2\Omega\cos\theta_j v_{kj} = 0. \tag{58}$$

Substituting u_{kj}, v_{kj} from (52) - (53) in (57) - (58) one obtains (similar to (26) - (27))

$$\left(\frac{\partial}{\partial t}\nabla^2 + 2\Omega\delta_p\right)\Phi_{kj} + 2\Omega\left(\sin\theta_j\nabla^2 + \cos\theta_j\delta_q\right)\Psi_{kj} + \frac{g}{a}\nabla^2 h_{kj} = 0 \tag{59}$$

$$\left(\frac{\partial}{\partial t}\nabla^2 + 2\Omega\delta_p\right)\Psi_{kj} - 2\Omega\left(\sin\theta_j\nabla^2 + \cos\theta_j\delta_q\right)\Phi_{kj} = 0. \tag{60}$$

[†]This means that we have to evaluate (36) at the point $k+p/2\;j$ instead of $k\;j$ and similarly for the other terms in this equation and next

Equation (38) can also be written (to second order in $q\Delta\theta$)

$$
\begin{aligned}
\frac{\partial h_{kj}}{\partial t} = -\frac{H}{a} \quad & \left\{ \frac{1}{\cos^2\theta_j} \delta_{2p}\delta_p \Phi_{k\,j} \right. \\
& + \frac{1}{\cos\theta_j} \delta_{2q} \left(\cos\theta_j \delta_q \Phi_{k\,j} \right) \\
& \left. + \frac{1}{\cos\theta_j} \left(\delta_{2p}\delta_q - \delta_{2q}\delta_p \right) \Psi_{k\,j} \right\} .
\end{aligned} \tag{61}
$$

Note that (61) is slightly different from (25). The first two terms would combine to $\nabla^2\Phi_{k\,j}$ if we had δ_p, δ_q instead of δ_{2p}, δ_{2q}, respectively. In this case, the third term would then vanish. It may be easier to rewrite (61) as follows

$$
\begin{aligned}
\frac{\partial h_{kj}}{\partial t} = -\frac{H}{a} \quad & \left\{ \nabla^2 \Phi_{kj} + \frac{1}{\cos^2\theta_j} (\delta_{2p} - \delta_p) \delta_p \Phi_{kj} \right. \\
& + \frac{1}{\cos\theta_j} (\delta_{2q} - \delta_q)(\cos\theta_j \delta_q \Phi_{k\,j}) \\
& \left. + \frac{1}{\cos\theta_j} \left(\delta_{2p}\delta_q - \delta_{2q}\delta_p \right) \Psi_{k\,j} \right\}
\end{aligned} \tag{62}
$$

where the first term is now the same as (25) and the others represent the perturbation. <u>These other terms actually suggest that one should take $u_{k\pm p/2\;j}$, $v_{k\;j\pm q/2}$ in (38), i.e. staggering the variable h</u>. In this case (36)-(37) should also change. We now rewrite (36)-(38) for the staggered grid (semidiscrete staggered Turkel Zwas scheme)

$$
\left.\frac{\partial u}{\partial t}\right|_{k,j} = -\frac{1}{a\Delta\lambda} \, \frac{g}{p\cos\theta_j} \left(h_{k+p/2,j} - h_{k-p/2,j} \right) + f_j \left[(1-\alpha) v_{k,j} + \frac{\alpha}{2} \left(v_{k+p,j} + v_{k-p,j} \right) \right] \tag{63}
$$

$$
\left.\frac{\partial v}{\partial t}\right|_{k,j} = -\frac{1}{a\Delta\theta} \, \frac{g}{q} \left(h_{k,j+q/2} - h_{k,j-q/2} \right) - \left[(1-\alpha) f_j u_{k,j} + \frac{\alpha}{2} \left(f_{j+q} u_{k,j+q} + f_{j-q} u_{k,j-q} \right) \right] \tag{64}
$$

$$
\begin{aligned}
\left.\frac{\partial h}{\partial t}\right|_{kj} = & -\frac{1}{a}\frac{H}{\cos\theta_j}\left[(1-\alpha)\left(\frac{u_{k+p/2,j}-u_{k-p/2,j}}{p\Delta\lambda}+\frac{v_{k,j+q/2}\cos\theta_{j+q/2}-v_{k,j-q/2}\cos\theta_{j-q/2}}{q\Delta\theta}\right)\right.\\
& +\frac{\alpha}{2}\left(\frac{u_{k+p/2,j+q/2}-u_{k-p/2,j+q/2}}{p\Delta\lambda}+\frac{u_{k+p/2,j-q/2}-u_{k-p/2,j-q/2}}{p\Delta\lambda}\right.\\
& +\frac{v_{k+p/2,j+q/2}\cos\theta_{j+q/2}-v_{k+p/2,j-q/2}\cos\theta_{j-q/2}}{q\Delta\theta}\\
& \left.\left.+\frac{v_{k-p/2,j+q/2}\cos\theta_{j+q/2}-v_{k-p/2,j-q/2}\cos\theta_{j-q/2}}{q\Delta\theta}\right)\right].
\end{aligned}
\tag{65}
$$

Thus (42)-(43) become

$$
-icu_{kj} = -\frac{g}{2a}im\hat{\eta}\frac{h_{kj}}{\cos\theta_j}+f_j\rho v_{kj} \tag{66}
$$

$$
-icv_{kj} = -\frac{g}{2a}\frac{\partial h_{kj}}{\partial\theta}-f_j u_{kj} \tag{67}
$$

where

$$
\hat{\eta} = \frac{\sin\frac{mp\Delta\lambda}{2}}{\frac{mp\Delta\lambda}{2}}. \tag{68}
$$

Equations (66)-(67) can be solved for u_{kj} and v_{kj}, thus

$$
u_{kj} = \frac{g}{2a}\frac{1}{2\Omega Q(\theta_j)}\left[m\Lambda\hat{\eta}\sec\theta_j+\rho\sin\theta_j\frac{\partial}{\partial\theta}\right]h_{kj} \tag{69}
$$

$$
v_{kj} = -i\frac{g}{2a}\frac{1}{2\Omega Q(\theta_j)}\left[m\hat{\eta}\tan\theta_j+\Lambda\frac{\partial}{\partial\theta}\right]h_{kj}. \tag{70}
$$

The equivalent of (49) is now

$$
-ich_{kj} = -\frac{H}{2a\cos\theta_j}\left[im\hat{\eta}\,u_{kj}+\hat{\rho}\frac{\partial}{\partial\theta}\left(v_{kj}\cos\theta_j\right)\right] \tag{71}
$$

where

$$
\hat{\rho} = 1-\alpha+\alpha\cos m\frac{p}{2}\Delta\lambda. \tag{72}
$$

Equations (59) - (60) are not affected (to second order in $q\Delta\theta$) by the staggering. Equation (62) simplifies to

$$
\frac{\partial h_{kj}}{\partial t} = -\frac{H}{a}\nabla^2\Phi_{kj}. \tag{73}
$$

We seek solutions to (59) - (60) and (73) proportional to e^{-ict} where c denotes the radian frequency. These equations become

$$
\left(\Lambda\nabla^2+i\delta_p\right)\Phi_{kj}+\left(\mu\nabla^2+\sqrt{1-\mu^2}\delta_q\right)i\Psi_{kj} = -i\frac{g}{2a\Omega}\nabla^2 h_{kj} \tag{74}
$$

$$\left(\Lambda\nabla^2 + i\delta_p\right)\Psi_{kj} - \left(\mu\nabla^2 + \sqrt{1-\mu^2}\delta_q\right) i\Phi_{kj} = 0 \tag{75}$$

$$h_{kj} = -\frac{Hi}{ac}\nabla^2\Phi_{kj}. \tag{76}$$

Eliminating h_{kj} from (74) by using (76) we have

$$\left(\Lambda\nabla^2 + i\delta_p + \frac{1}{\epsilon\Lambda}\nabla^4\right)\Phi_{kj} + \left(\mu\nabla^2 + \sqrt{1-\mu^2}\delta_q\right) i\Psi_{kj} = 0 \tag{77}$$

$$\left(\mu\nabla^2 + \sqrt{1-\mu^2}\delta_q\right) i\Phi_{kj} - \left(\Lambda\nabla^2 + i\delta_p\right)\Psi_{kj} = 0. \tag{78}$$

Suppose Φ_{kj}, Ψ_{kj} depend on λ_k in the following way,

$$\Phi_{kj} = F_j e^{im\lambda_k} \tag{79}$$

$$\Psi_{kj} = G_j e^{im\lambda_k} \tag{80}$$

where m is a nonnegative integer, then

$$\delta_q\Psi_{k\,j} = \delta_q G_j e^{im\lambda_k} = \frac{G_{j+q/2} - G_{j-q/2}}{q\Delta\theta} e^{im\lambda_k} \tag{81}$$

$$\delta_p\Phi_{kj} = im\hat{\eta}F_j e^{im\lambda_k} \tag{82}$$

and

$$\nabla^2\Phi_{kj} = \left[\frac{-(m\hat{\eta})^2}{1-\mu^2} + \frac{1}{\sqrt{1-\mu^2}}\delta_q(\sqrt{1-\mu^2}\delta_q)\right] F_j e^{im\lambda_k}. \tag{83}$$

Upon substituting (82) in (77) - (78), we get the semi-discrete analog of (31) and (29), respectively.

3.3 Comparison of Discrete and Continuous Modal Expansion

In this subsection, we compare the equations used for the modal expansion in the continuous case, i.e. (31) and (29) with the corresponding ones for the Turkel Zwas discretization. These equations for the staggered Turkel Zwas scheme are (77)-(78), respectively. In the unstaggered case, we were unable to obtain such a system, since (61) is different in form from (25). This difference led us to the development of the staggered scheme.

Notice the similarity between (77) and (31). The operator ∇^2, as defined immediately after (30), in (31) is replaced by its discrete analog defined in (56). The operator $D = (1-\mu^2)\frac{\partial}{\partial\mu}$ is now discretized by $\sqrt{1-\mu^2}\delta_q$. The discrete operator $i\delta_p$ becomes $-m$ in the continuous case. The same analogy holds between (29) and (78).

4 STAGGERED TURKEL-ZWAS SCHEME

As was shown in the previous section, it is necessary to stagger the grid. The staggered version of the Turkel-Zwas scheme takes the following form:

$$\begin{aligned}
u_{k,j}^{\ell+1} = u_{k,j}^{\ell-1} \quad & -\sigma\Big[\tfrac{u_{k,j}^{\ell}}{\cos\theta_j}(u_{k+1,j}^{\ell} - u_{k-1,j}^{\ell}) + v_{k,j}^{\ell}(u_{k,j+1}^{\ell} - u_{k,j-1}^{\ell}) \\
& +\tfrac{2g}{p\cos\theta_j}(h_{k+\frac{p}{2},j}^{\ell} - h_{k-\frac{p}{2},j}^{\ell})\Big] \\
& +2\Delta t\Big[(1-\alpha)(f_j + \tfrac{u_{k,j}^{\ell}}{a}\tan\theta_j)v_{k,j}^{\ell} \\
& +\tfrac{\alpha}{2}(f_j + \frac{u_{k+\frac{p}{2},j}^{\ell}}{a}\tan\theta_j)v_{k+\frac{p}{2},j}^{\ell} \\
& +\tfrac{\alpha}{2}(f_j + \frac{u_{k-\frac{p}{2},j}^{\ell}}{a}\tan\theta_j)v_{k-\frac{p}{2},j}^{\ell}\Big]
\end{aligned} \tag{84}$$

$$\begin{aligned}
v_{k,j}^{\ell+1} = v_{k,j}^{\ell-1} \quad & -\sigma\Big[\tfrac{u_{k,j}^{\ell}}{\cos\theta_j}\left(v_{k+1,j}^{\ell} - v_{k-1,j}^{\ell}\right) + v_{k,j}^{\ell}\left(v_{k,j+1}^{\ell} - v_{k,j-1}^{\ell}\right) \\
& +\tfrac{2g}{q}\left(h_{k,j+\frac{q}{2}}^{\ell} - h_{k,j-\frac{q}{2}}^{\ell}\right)\Big] \\
& -2\Delta t\Big[(1-\alpha)\left(f_j + \tfrac{u_{k,j}^{\ell}}{a}\tan\theta_j\right)u_{k,j}^{\ell} \\
& +\tfrac{\alpha}{2}\left(f_{j+\frac{q}{2}} + \frac{u_{k,j+\frac{q}{2}}^{\ell}}{a}\tan\theta_{j+\frac{q}{2}}\right)u_{k,j+\frac{q}{2}}^{\ell} \\
& +\tfrac{\alpha}{2}\left(f_{j-\frac{q}{2}} + \frac{u_{k,j-\frac{q}{2}}^{\ell}}{a}\tan\theta_{j-\frac{q}{2}}\right)u_{k,j-\frac{q}{2}}^{\ell}\Big]
\end{aligned} \tag{85}$$

$$
\begin{aligned}
h_{k,j}^{\ell+1} = h_{k,j}^{\ell-1} \quad & -\sigma \left\{ \frac{u_{k,j}^{\ell}}{\cos\theta_j} \left(h_{k+1,j}^{\ell} - h_{k-1,j}^{\ell} \right) + v_{k,j}^{\ell} \left(h_{k,j+1}^{\ell} - h_{k,j-1}^{\ell} \right) \right. \\
& + \frac{2h_{k,j}^{\ell}}{\cos\theta_j} \left[(1-\alpha) \left(u_{k+\frac{p}{2},j}^{\ell} - u_{k-\frac{p}{2},j}^{\ell} \right) \right. \\
& \left. + \frac{\alpha}{2} \left(u_{k+\frac{p}{2},j+\frac{q}{2}}^{\ell} - u_{k-\frac{p}{2},j+\frac{q}{2}}^{\ell} + u_{k+\frac{p}{2},j-\frac{q}{2}}^{\ell} - u_{k-\frac{p}{2},j-\frac{q}{2}}^{\ell} \right) \right] \frac{1}{p} \\
& + \frac{2h_{k,j}^{\ell}}{\cos\theta_j} \left[(1-\alpha) \left(v_{k,j+\frac{q}{2}}^{\ell} \cos\theta_{j+\frac{q}{2}} - v_{k,j-\frac{q}{2}}^{\ell} \cos\theta_{j-\frac{q}{2}} \right) \right. \\
& + \frac{\alpha}{2} \left(v_{k+\frac{p}{2},j+\frac{q}{2}}^{\ell} \cos\theta_{j+\frac{q}{2}} - v_{k+\frac{p}{2},j-\frac{q}{2}}^{\ell} \cos\theta_{j-\frac{q}{2}} \right. \\
& \left. \left. \left. + v_{k-\frac{p}{2},j+\frac{q}{2}} \cos\theta_{j+\frac{q}{2}} - v_{k-\frac{p}{2},j-\frac{q}{2}} \cos\theta_{j-\frac{q}{2}} \right) \right] \frac{1}{q} \right\}
\end{aligned}
\tag{86}
$$

where σ is given by (35). If p and q are even integers, the staggered grid does not require any intermediate values. In figure 1, we show the location of the grid points used by the unstaggered Turkel-Zwas scheme in each of the equations (for $p = q = 3$.) For the staggered grid (again $p = q = 3$) intermediate values are required for h in the momentum equation and for u and v in the continuity equation. It is interesting to see the difference between the staggered grid with $p = q = 2$ and the unstaggered grid with $p = q = 1$. One may feel that if we have $p/2$, $q/2$ instead of p, q respectively, the two above mentioned grids are the same. The truth is that in the momentum equation only h moves closer to the center, and thus the grids are different, see figure 2. In the h equation, both u and v move closer to the center and the staggered grid with $p = q = 2$ is now the same as the unstaggered grid with $p = q = 1$, see figure 3. Note that the grid for the h equation is identical to that in figure 2 and thus not repeated.

5 NUMERICAL RESULTS

In this section we present the numerical results for the unstaggered and staggered versions of the Turkel-Zwas scheme. The initial conditions are the same as those used by McDonald and Bates[14] where the height is defined as follows

$$h(\lambda,\theta,0) = \frac{1}{g}(\bar{\Phi} + 2\Omega a u_o \sin^3\theta\cos\theta\sin\lambda)$$

and the velocities are obtained geostrophically to yield

$$u(\lambda,\theta,0) = -3u_o\sin\theta\cos^2\theta\sin\lambda + u_o\sin^3\sin\lambda$$

$$v(\lambda,\theta,0) = u_o\sin^2\theta\cos\lambda$$

where

$$g = 9.8\frac{\mathrm{m}}{\mathrm{sec}^2}$$

$$\bar{\Phi} = 5.768\times 10^4\frac{\mathrm{m}^2}{\mathrm{sec}^2}$$

$$u_o = 20\frac{\mathrm{m}}{\mathrm{sec}}$$

$$a = 6.370\times 10^6\ \mathrm{m}$$

$$\Omega = 7.292\times 10^{-5}\frac{\mathrm{rad}}{\mathrm{sec}}.$$

The ℓ^2 error norms for the height and velocity are computed in the following manner

$$||h||_{\ell^2} = \frac{\sqrt{I[(h(\lambda,\theta)-h_e(\lambda,\theta))^2]}}{\sqrt{I[(h_e(\lambda,\theta))^2]}}$$

and

$$||\underline{u}||_{\ell^2} = \frac{\sqrt{I[(u(\lambda,\theta)-u_e(\lambda,\theta))^2 + (v(\lambda,\theta)-v_e(\lambda,\theta))^2]}}{\sqrt{I[(u_e(\lambda,\theta))^2+(v_e(\lambda,\theta))^2]}}$$

where

$$I[f(\lambda,\theta)] = \frac{1}{4\pi}\int_0^{2\pi}\int_{-\frac{\pi}{2}}^{\frac{\pi}{2}} f(\lambda,\theta)\cos\theta\, d\theta\, d\lambda.$$

In these relations the variables h_e, u_e, and v_e are considered to be the exact solution. This solution is obtained by a centered in space and time algorithm (a leapfrog scheme) on a 128×64 grid that is time integrated using a time step of 15 seconds. The height at the initial ($t = 0$ hours) and final ($t = 24$ hours) states are shown in figures 4 and 5. The percent change in total available energy is defined as

$$\Delta E = \frac{I[E_{final}] - I[E_{initial}]}{I[E_{initial}]} \times 100\%$$

where

$$E(\lambda, \theta) = \frac{1}{2}[h(\lambda, \theta)(u(\lambda, \theta)^2 + v(\lambda, \theta)^2) + (h(\lambda, \theta) - \frac{\bar{\Phi}}{g})^2].$$

The shallow water equations are integrated in time for a period of 24 hours on a 64×32

Staggered Grid	p	q	α	Δt (sec)	$\|\|h\|\|_{\ell^2}$ ($\times 10^{-4}$)	$\|\|u\|\|_{\ell^2}$ ($\times 10 - 3$)	ΔE (%)	CPU (sec)
No	1	1	0	100	1.177	3.722	-0.09	240
No	2	1	1/3	200	1.187	3.830	-0.06	119
No	3	2	1/3	200	2.367	8.018	-0.15	119
Yes	3	2	1/3	200	1.221	4.096	-0.03	119
No	4	2	1/3	200	2.406	8.387	-0.15	119
Yes	4	2	1/3	200	1.269	4.478	0	119
No	3	1	1/3	300	1.193	3.931	-0.06	83
No	5	2	1/3	300	2.475	8.844	-0.15	83
Yes	5	2	1/3	300	1.344	5.081	+0.03	83
No	6	2	1/3	300	2.592	9.471	-0.15	83
Yes	6	2	1/3	300	1.467	5.977	+0.06	83
No	4	1	1/3	400	1.211	4.149	-0.06	61
No	7	2	1/3	400	2.735	10.06	-0.15	61
Yes	7	2	1/3	400	1.634	7.131	+0.09	61
No	8	2	1/3	400	2.881	10.90	-0.15	61
Yes	8	2	1/3	400	1.871	8.585	+0.15	61

Table 1: The ℓ^2 error norms for the height h and the velocity field u for the unstaggered and staggered versions of the Turkel-Zwas scheme for a 64×32 grid after 24 hours. The parameter ΔE represents the percent change of available energy of the system.

grid on a Sparc 10. Table 1 shows the results for various configurations of p and q using different time steps for the unstaggered and staggered versions of the Turkel-Zwas scheme. Recall that p and q refer to the extension of the differencing stencil in the longitudinal (λ) and latitudinal (θ) directions, respectively, and α is the Padé-type differencing weight. We have experimented with various values of α, namely $\alpha = 0, \frac{1}{4}, \frac{1}{3}, \frac{1}{2}, \frac{2}{3}, \frac{3}{4}, 1$. We have found that $\alpha = \frac{1}{3}$ is the best choice. The first row in table 1 represents the leapfrog scheme which only allows a time step of 100 seconds due to the very restrictive CFL condition which limits all explicit algorithms. For the remainder of the cases, p is always greater than q because the time restriction is dictated by the distance between mesh points in the λ direction. As p increases so too does the maximum allowable time step because the CFL restriction is relaxed due to the coarser differencing stencil used for the gravity wave terms. For typical meteorological conditions the inertial gravity wave speeds are larger than the wind velocities while most of the energy is carried by the wind velocities. Thus it makes sense to treat the gravity terms less accurately by using a coarser grid for these terms (see Turkel and Zwas[1]).

Table 1 shows that for the lower values of p and q, say (p=2,q=1) for the unstaggered and (p=3,q=2) for the staggered and Δt = 200, the unstaggered and staggered cases yield comparable error norms. As p and q are increased beyond these values, the errors increase dramatically for the unstaggered case; the errors for the staggered case are only half those of the unstaggered case. Note that for the same time step, the staggered case takes no more CPU time than the unstaggered case. In addition, the staggered case where (p=4, q=2) conserves the total available energy. As p increases, the staggered case no longer conserves the available energy but it is still more accurate than the unstaggered case for the same values of p and q. Therefore for the staggered case the optimal values of p and q must lie somewhere in the vicinity of (p=3,q=2) and (p=4, q=2). By comparing the error norms for the unstaggered case for the values (p=3, q=1) and (p=3, q=2), and (p=4,q=1) and (p=4,q=2) we see that the increase in q from 1 to 2 has adverse effects on the solution accuracy. Therefore it stands to reason that for the staggered case a better solution can be achieved by the values (p=3,q=1) or (p=4, q=1). The difficulty with this case is that now interpolation is required because the staggering for odd values of p and q results in intermediate values. Intermediate values in the longitudinal direction pose no difficulty and in fact are handled by linear interpolation in this paper. On the other hand, intermediate values in the latitudinal direction cause problems because interpolation is now required at the poles where the wind velocities are undefined. This case is not included in this paper.

For completeness let us review the case Δt = 200 once again. The staggered case (p=4,q=2) yields better results than the unstaggered case (p=4, q=2). However, the unstaggered case allows a time step of 400 seconds. The staggered case, on the other hand, cannot use as large a time step because the CFL condition is dictated by terms using the differencing stencil points (p/2, q/2) instead of (p,q). This means that there is a trade-off between computing time and accuracy; for a given value of p and q, the unstaggered case allows a larger time step than the staggered case thereby requiring less CPU time at the cost of lower accuracy. To clarify the point, we recall that Song and Tang have proved that basically the stability condition of the unstaggered case is

$$\frac{\Delta}{d} = \frac{p}{\sqrt{2gh}}.$$

Since in our case, we have the points half way the original (unstaggered) distance, we replace the numerator by $\frac{p}{2}$ or, which is the same as halving the value of $\frac{\Delta t}{d}$. For the spherical case, similar dependence was proved by Turkel and Zwas[1] (see our introduction).

6 SUMMARY AND CONCLUSIONS

The analysis of the spherical coordinates shallow water equations model shows that the T-Z scheme must be staggered to get eigenvalues and eigenfunctions approaching those of the continuous case. The importance of such an analysis is the fact that it is valid for non-constant coefficients and thereby applicable to any numerical scheme. In addition, numerical experiments are conducted illustrating the benefits of staggering the original scheme. The numerical experiments show that for given values of p and q the staggered case performs better than the unstaggered case. However, the staggered case requires half the time step of the unstaggered case. This means that there is a trade-off between efficiency and accuracy; for a given value of p and q, the unstaggered case allows a larger time step than the staggered case thereby requiring less CPU time at the cost of lower accuracy. These experiments also show that the best results for the staggered case are obtained with the values $(p = 3, q = 2)$ and $(p = 4, q = 2)$. Furthermore, the experiments suggest that better results may be obtained by the configurations $(p = 3, q = 1)$ and $(p = 4, q = 1)$ but interpolation is required in the latitudinal direction because odd values of p or q result in differencing points that do not lie on grid points (intermediate values). Interpolation in the longitudinal direction is straight-forward and is handled by linear interpolation in this paper, while in the latitudinal direction it is no longer trivial because intermediate values may fall on the poles where the wind velocities are undefined.

Software for both the unstaggered and staggered Turkel Zwas schemes for the approximation of the shallow water equations in spherical coordinates is available at URL address http://math.nps.navy.mil/$\sim$ bneta.

ACKNOWLEDGEMENTS

This research was conducted for the Office of Naval Research and was funded by the Naval Postgraduate School. The algebraic manipulations were checked by Chris Sagovac using MACSYMA on the VAX at the Electrical and computer Engineering Department. We are grateful to the referees' and editor's comments which improved the presentation. The second author (FXG) would like to acknowledge the support of the National Research Council, the Naval Postgraduate School and the Naval Research Laboratory.The third author (IMN) was partially supported by the Supercomputer Computations Research Institute which is partially funded by the U.S. Department of Energy through contract No. DE-FC05-85ER250000.

REFERENCES

1. E. Turkel and G. Zwas, Explicit large time-step schemes for the shallow water equations, in *Advances in Computer Methods for Partial Differential Equations*, R. Vichnevetsky and R.S. Stepleman (eds), IMACS, Lehigh University, 65–69 (1979).

2. A. L. Schoenstadt, A transfer function analysis of numerical schemes used to simulate geostrophic adjustment, *Mon. Wea. Rev.*, **108**, 1248–1259 (1980).

3. B. Neta and I. M. Navon, Analysis for the Turkel-Zwas scheme for the shallow water equations, *J. Comp. Phys.*, **81**, 277–299 (1989).

4. B. Neta and C. L. DeVito, The transfer function analysis of various schemes for the two dimensional shallow water equations, *Comp. Math. Applics.*, **16**, 111–137 (1988).

5. I. M. Navon and R. deVilliers, The application of the T-Z explicit large time step scheme to a hemispheric barotropic model with constraint restoration, *Mon. Wea. Rev.*, **115**, 1036–1051 (1987).

6. Navon, I. M., and Yu, J., EXSHALL - A Turkel-Zwas large-time step explicit Fortran program for solving the shallow-water equations on the sphere, *Computers and Geosciences*, **17**, 1311–1343 (1991).

7. F. G. Stremler, *Introduction to Communication Systems*, Addison-Wesley Pub. Co., Reading, MA 1977.

8. J. Steppeler, Analysis of group velocities of various finite element schemes, *Beitr. Phys. Atmosph.*, **62**, 151–161 (1989).

9. J. Steppeler, I. M. Navon and H. -I. Lu, Finite element schemes for extended integration of atmospheric models, *J. Comp. Phys.*, **89**, (1990). 95–124.

10. B. Neta, Analysis of the Turkel-Zwas scheme for the 2-D shallow water equations, IMACS *Transactions on Scientific Computing 1988, Vols. 1.1 and 1.2: Numerical and Applied Mathematics*, W. F. Ames and C. Brezinski (eds.) 1989.

11. J. Pedlosky, *Geophysical Fluid Dynamics,* Springer Verlag, New York, 1979.

12. M. S. Longuet-Higgins, The Eigenfunctions of Laplace's Tidal Equations Over a Sphere, *Phil. Trans. Royal Soc. London,* **A262**, (1968), 511–607.

13. Y. Song and T. Tang, On staggered Turkel-Zwas schemes for two-dimensional shallow water equations, *Monthly Weather Review*, **122**, (1994), 223–234.

14. A. McDonald and J. R. Bates, Semi-Lagrangian Integration of a Gridpoint Shallow Water Model on the Sphere, *Monthly Weather Review*, **117**, (1989), 130–137.

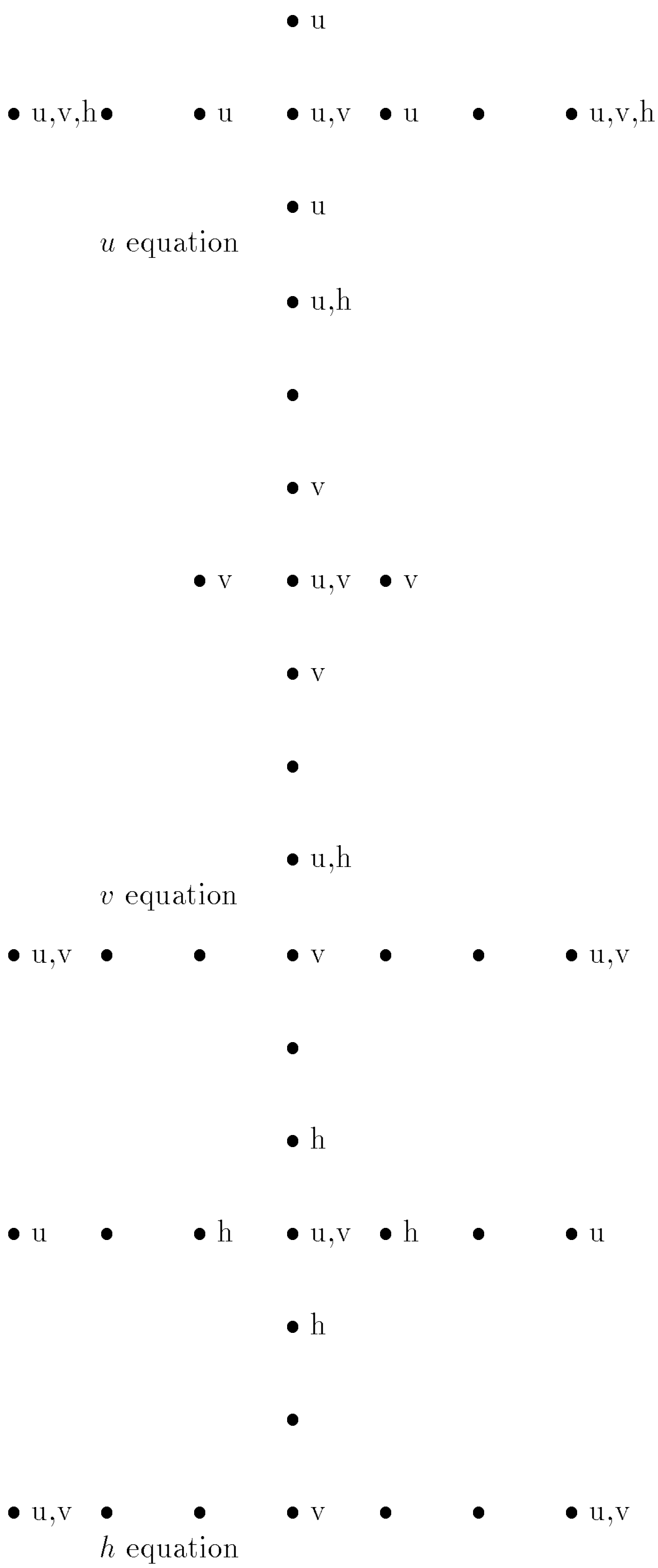

Figure 1: Unstaggered Grid with $p = q = 3$

• u

• u,v • u,h • u,v • u,h • u,v

• u

u equation

• u

• v,h

• v • u,v • v

• v,h

• u

v equation

• u,v • v,h • u,v

• u,h • u,v • u,h

• u,v • v,h • u,v

h equation

Figure 2: Staggered Grid with $p = q = 2$

• u

• u,v,h • u,v • u,v,h

• u

u equation

• u,v,h

• v • u,v • v

• u,v,h

v equation

Figure 3: Unstaggered Grid with $p = q = 1$

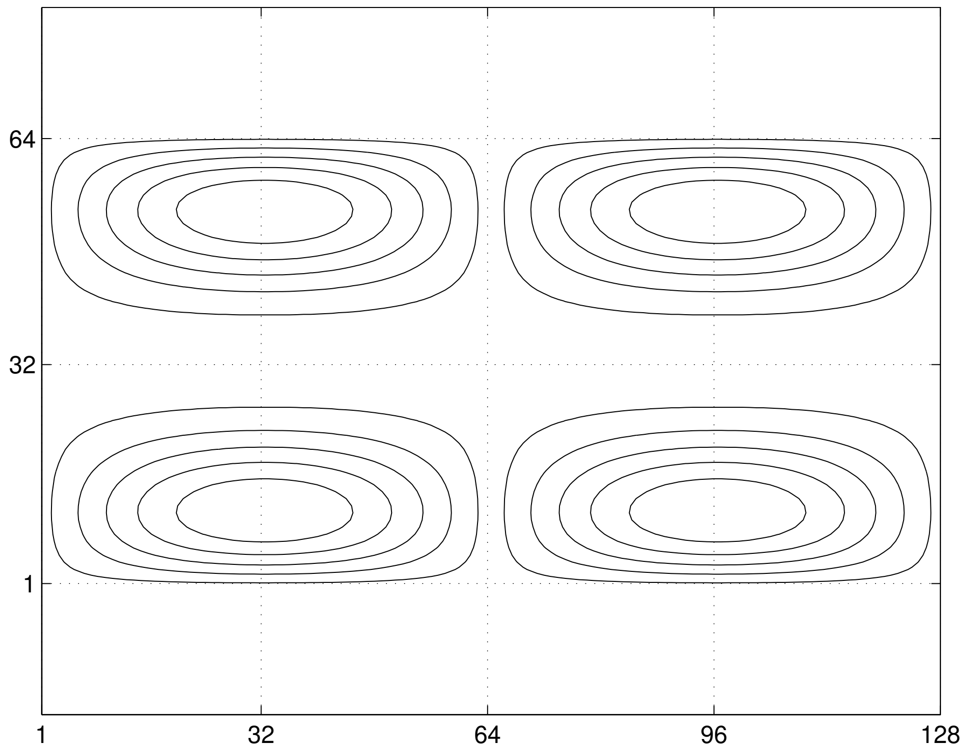

Figure 4: The height at the initial state ($t = 0$ hours). The grid is 128×64.

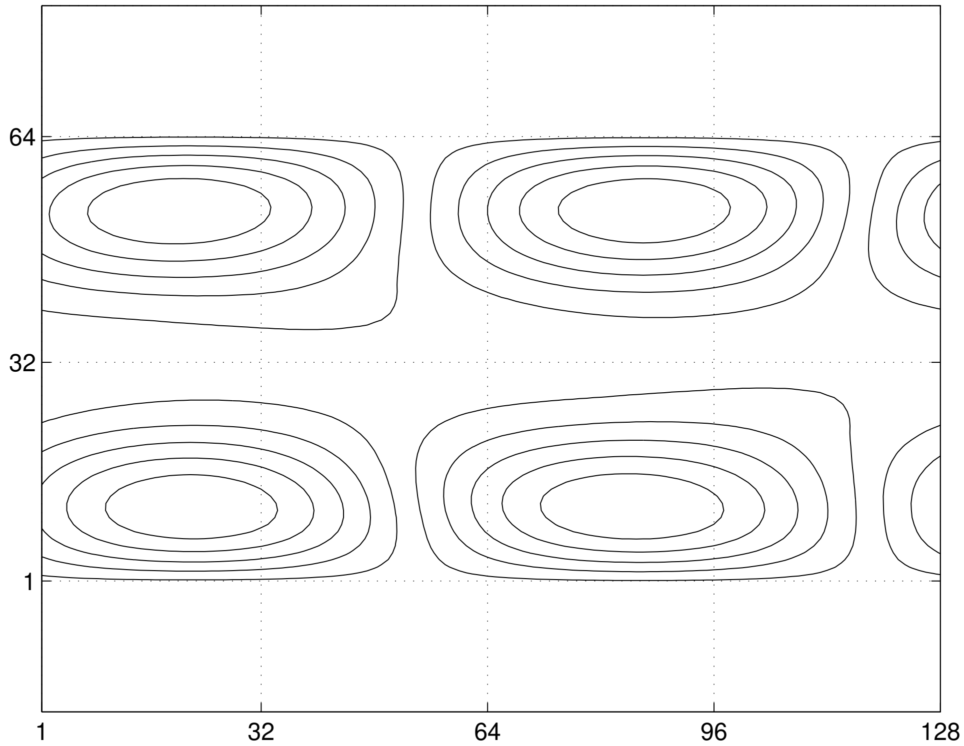

Figure 5: The height at the final state (t = 24 hours). The grid is 128×64 and the time step is $\Delta t = 15$ seconds.